Direct Microscopic Study of Doubly Polarized Atomic Hydrogen by Electron-Spin Resonance

G. H. van Yperen, Isaac F. Silvera,[a] J. T. M. Walraven, J. Berkhout, and J. G. Brisson[a]
Natuurkundig Laboratorium, University of Amsterdam, 1018XE Amsterdam, The Netherlands
(Received 5 October 1982)

By means of ESR in a high magnetic field the hyperfine states of a gas of spin-polarized atomic hydrogen are directly probed. This allows a direct determination of the spin-state populations and nuclear polarization. The unusual ESR line shape is attributed to field inhomogeneities. The temperature of the gas was determined by use of ESR with no indication of nonequilibrium due to Kapitza resistance. Recombination rates between hyperfine states could be determined.

PACS numbers: 67.40.-w, 67.70.+n

The hydrogen atom in a high magnetic field, B, has four distinct hyperfine spin states: the two lower ones $|a\rangle = |\downarrow\uparrow\rangle - \epsilon|\uparrow\downarrow\rangle$, $|b\rangle = |\downarrow\downarrow\rangle$ and the two upper ones $|c\rangle = |\uparrow\downarrow\rangle + \epsilon|\downarrow\uparrow\rangle$, $|d\rangle = |\uparrow\uparrow\rangle$. Here the arrow and the crossed arrow represent the projections of the electron and nuclear spins, respectively, and $\epsilon \approx a/4\mu_B B$ is the mixing parameter where a is the hyperfine constant and μ_B the Bohr magneton.[1] The recently stabilized gas of electron-spin-polarized atomic hydrogen ($H^{\downarrow}$) is a mixture of states $|a\rangle$ and $|b\rangle$,[2] whereas electron and nuclear polarized hydrogen ($H^{\downarrow\downarrow}$) is a gas of $|b\rangle$-state atoms.[3,4] Magnetic dipole transitions, allowed for $|a\rangle \rightarrow |d\rangle$ and $|b\rangle \rightarrow |c\rangle$, are separated in field by 506.8 G.

Until now all information concerning the populations of the hyperfine states in high field has been implied from the decay of the gas pressure as a function of time. In this Letter we report on the first detailed microscopic investigation of the evolution in time of the populations of the two lower hyperfine states using a microwave transmission cell to perform ESR.[5] We show that because of magnetic field inhomogeneities, the ESR line has a complex shape which can be explained by a simple model. With a special magnetic field profile, this technique can be used to study the density profile and thus the condensate fraction in a Bose condensed gas of hydrogen.[6] Additionally, knowledge of these results is vital, for example, for proposed proton scattering experiments at CERN in which atomic hydrogen, stabilized by the technique used here, would be pulsed into the accelerator beam by ESR techniques.[7] By plotting the density as determined by ESR versus that determined with a pressure gauge, we have studied the deviations from thermal equilibrium due to Kaptiza thermal resistance, and do not find an equilibrium problem. We have also developed an alternative means to that of Sprik *et al.*[4] for measuring the rate constants $K_{aa}{}^{e}$ and $K_{ab}{}^{e}$ where $K_{ij}{}^{e}$ is the recombination rate constant of i-state and j-state atoms interacting on the helium surface, and find agreement with their measurements.

We have developed the hybrid system of far-infrared (FIR) light-pipe optics and high-resolution microwave electronics shown in Fig. 1. In this design we sacrifice the sensitivity of a high-Q cavity for a single-pass broadband cell which

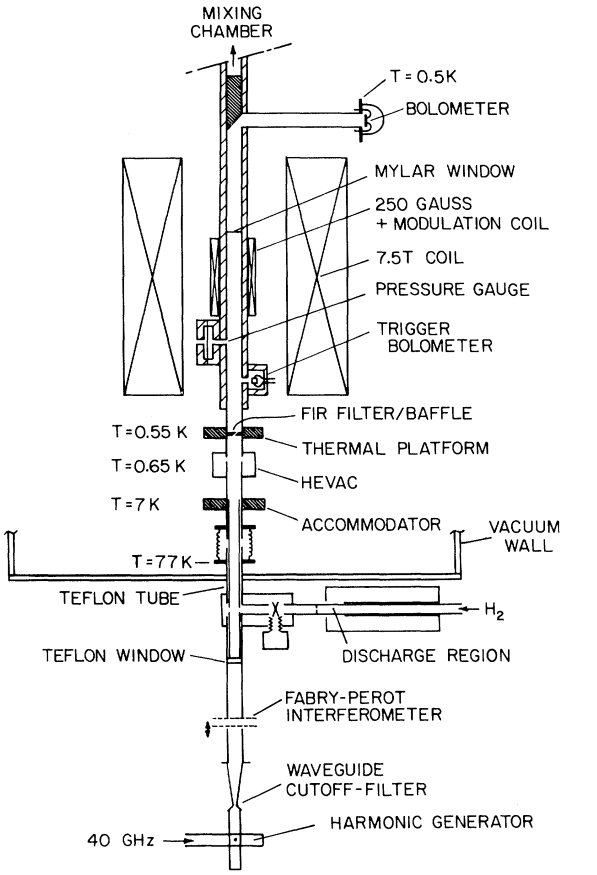

FIG. 1. The experimental system for ESR. Cryogenic details concerning the HEVAC, accommodator, etc., can be found in Ref. 1.

has sufficient sensitivity to detect the absorption and which can ultimately be used to study the density profiles of hydrogen or deuterium. The cell is also equipped with a strain gauge and a trigger bolometer for measuring the H pressure and for destroying (recombining) the H sample.[1] The ESR cell is a long copper tube of 5 mm i.d. in a magnetic field with homogeneity of 1 in 10^5 in a 1-cm-diam sphere. Hydrogen from a discharge fills the cell whose walls are coated by a thin film of ^{4}He which suppresses surface recombination and is stabilized by now well-known techniques described elsewhere.[1] The H↓ gas which is bounded above by a Mylar window is confined to the high-field region by magnetic compression.[1,6] Microwave radiation is coupled in through the hydrogen fill tube. The microwave frequency is ≈ 160 GHz corresponding to a resonance field of ≈ 5.7 T. The 160-GHz signal is generated by feeding a harmonic multiplier with approximately 50 mW from a stabilized (1:10^7) 40-GHz source and using the fourth harmonic, having power at the detector of order 1 μW. Lower harmonics are rejected by using a waveguide beyond cutoff; higher, by means of an in-line wire-mesh Fabry-Perot etalon. Radiation transmitted through the H sample is detected with a far-infrared bolometer of the type described by Nishioka, Richards, and Woody[8] having noise-equivalent power of 10^{-13} W/Hz$^{1/2}$. The microwave signal can be modulated in frequency or amplitude, or by means of a small field $|B_1| \lesssim 250$ G used to shift between the two hyperfine transitions, or $|B_2| \lesssim 50$ G used for field modulation. A resonance line could be measured with a signal-to-noise ratio (S/N) of 1/Hz$^{1/2}$ for a density of 5.7×10^{13}/cm^3. Resonance in a region of strong absorption caused a measurable decrease in the gas density. The dominant loss mechanism is one in which atoms, flipped to the $|c\rangle$ or $|d\rangle$ states, are ejected from the cell by the magnetic field gradient. For a power of 10^{-8} W, we estimate the decay time constant to be 2×10^3 sec in our system. With a higher power we have been able to vary the polarization by pumping either the $|a\rangle$- or $|b\rangle$-state atoms out of the cell.

Since the intrinsic linewidth is very small, the line shape will be determined by field inhomogeneities. The energy absorption coefficient α is found by multiplying the transition probability by the energy per photon and the number of atoms in state i, $n_i(B)\Delta V$ (V is volume), at the resonance field, resulting in

$$\alpha = (\pi/4c)\mu_0\hbar\gamma^2 n_i(B)B/(\Delta B/\Delta Z) \text{ (mks)}. \quad (1)$$

Here we have assumed $n_c = n_d = 0$; γ is the gyromagnetic ratio. From this we see that the absorption will be strongest in regions where the gradient $\Delta B/\Delta Z \approx 0$. The underlying physics is the following: At low densities, $n_i \propto \exp(\mu_B B/kT)$ and is essentially constant for $\mu_B(B_{max} - B)/k \ll T$. Thus, in the (approximately) uniform field region, the line shape is determined by the field gradient only. Our field profile has a bump of ~5 G at a point above the uniform region but below

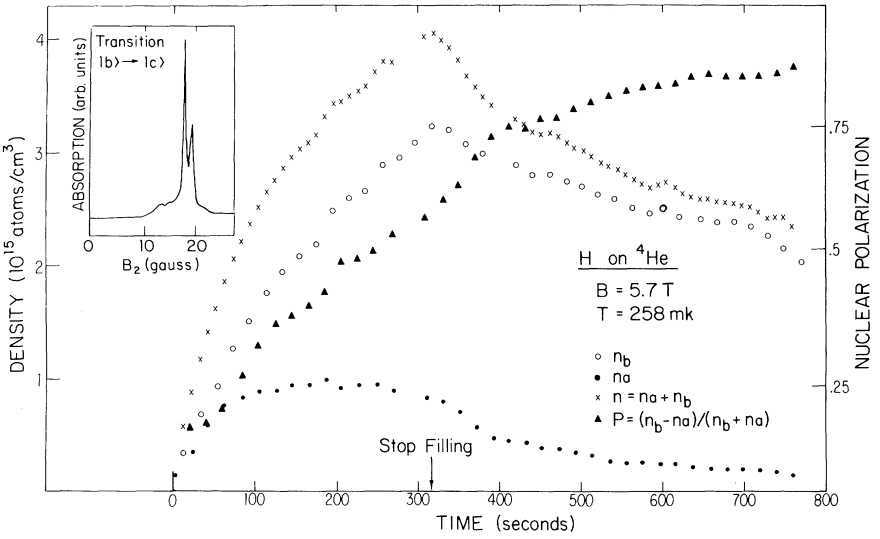

FIG. 2. The densities of the hyperfine states and polarization as measured by ESR. Inset: The ESR line shape as a function of the sweep field B_2, for one of the transitions.

the Mylar window so that the field has two zero-gradient regions. As a consequence each ESR transition is doubly peaked, as shown in the inset in Fig. 2. We have been able to simulate such line shapes using Eq. (1) and our known field profile. We note that to use the ESR line shape to determine the density profile as a means of detecting Bose-Einstein condensation as suggested by Walraven and Silvera,[6] it is useful to superimpose a field with a constant gradient $B_q = B_0 z$ with B_0 much greater than the nonuniformities in the main field. In this way, the line shape is directly proportional to the density profile, as seen from Eq. (1).

From Eq. (1) we see that the ESR signal, which is proportional to n_i, can be used as a direct measure of the state population and consequently the polarizability $P = (n_b - n_a)/(n_b + n_a)$. The evolution of the populations is shown in Fig. 2 under the specified conditions, during the filling and decay of the hydrogen in the cell. This provides the first direct demonstration that, as a result of selective recombination, H↓ transforms to H↓↓.

The ESR derivative signal was detected by frequency modulation, sweeping the main field through the resonance line in about 1 sec. This technique yielded the same shape for both ESR lines so that the peak values are proportional to n_i. A higher S/N ratio could be achieved with the modulation fields and multisweep averaging (see inset, Fig. 2); however, in this case the line shapes for the two lines differed as a result of the inhomogeneities in the fields B_1 and B_2 which are added or subtracted from the main field. Furthermore, the line shape changed with time because of a slow drift of the main field in persistent-mode operation (~2 G/h) which must be compensated for by B_1.

The rate equations for the decay of the density,[9] given, for example, in Ref. 4, are (with the shorthand notation $n_a \equiv a$, $n_b \equiv b$, and the assumption that filling flux, thermal leakage, and measurement losses are zero)

$$\dot{a} = -G_s{}^{ie}(a-b) - (G_v + G_s{}^{e})(a^2 - b^2) - 2K_{aa}{}^{e}a^2 - K_{ab}{}^{e}ab, \tag{2a}$$

$$\dot{b} = G_s{}^{ie}(a-b) + (G_v + G_s{}^{e})(a^2 - b^2) - K_{ab}{}^{e}ab, \tag{2b}$$

where $G_s{}^{ie}$, G_v, and $G_s{}^{e}$ are the surface impurity, volume, and intrinsic surface relaxation rates defined and discussed in Ref. 4. These are of no further explicit interest here as we shall eliminate them by adding Eqs. (2a) and (2b) to get an expression in terms of the effective surface recombination rates $K_{aa}{}^{e}$ and $K_{ab}{}^{e}$. Defining $n = a + b$ and $p' = b/a$, we find

$$-[(1+p')^2/2n^2]\,dn/dt = K_{aa}{}^{e} + K_{ab}{}^{e}p'. \tag{3}$$

Earlier methods[2,3] of determining rate constants from nonlinear least-squares fits to curves of the decay of pressure versus time were too insensitive to distinguish between $K_{aa}{}^{e}$ and $K_{ab}{}^{e}$. Sprik *et al.*[4] developed a boundary-value method. Now, with the ESR data, we can determine $K_{aa}{}^{e}/K_{ab}{}^{e}$ on a point-for-point basis using Eq. (3). The population ratio p' can be measured from the ESR signal and n as well as dn/dt from the pressure gauge ($n = p/kT$). An unweighted fit to the data points provided a value of 2.4, in agreement with the value of 2.23 ± 0.25 of Sprik *et al.*[4] However, systematic errors, apparent in the data, set greater margins of uncertainty. A fit ignoring systematic errors and using statistical weights yielded a value close to 8. It has been suggested[10] that the value of Sprik *et al.* would be larger if their H↓ sample was warmer than the cell walls as a result of Kapitza resistance between the H and helium. Our results cannot settle this question, but set a limit of 2–8 on $K_{aa}{}^{e}/K_{ab}{}^{e}$. In view of the systematic errors, we have a preference for the lower value.

Since the possible out-of-equilibrium warming of the H↓ seems to be a point of concern,[10] even for densities of order $1\times10^{16}/\mathrm{cm}^3$ used by Sprik *et al.*, we have devised a method of determining the gas temperature from the ESR signal. We

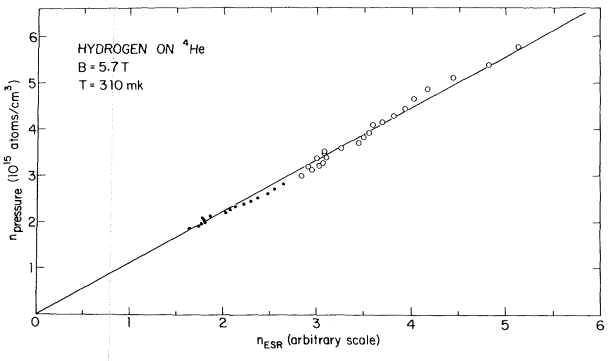

FIG. 3. The density of H↓ as measured by ESR and a pressure gauge. The linear relation indicates that the translational degrees of freedom of the gas are in thermodynamic equilibrium with the cell walls.

plot the density from the pressure measurement versus the sum of the $|a\rangle \rightarrow |d\rangle$ and $|b\rangle \rightarrow |c\rangle$ ESR signals, p/kT vs n_{ESR}, for $T = 310$ mK in Fig. 3. Deviations from equilibrium which would be expressed by deviations from a straight-line behavior are random and at most 14.5 mK. A systematic deviation at higher densities due to increasing heating, which is proportional to n^2, is absent. We thus establish that the Kapitza resistance is not yet a problem for the conditions studied.

We thank P. Wyder for suggesting the multiplier technique of generating the high-frequency microwave power, and H. A. Dijkerman for the loan of a klystron and stabilizer when ours malfunctioned. The technical help of O. Höpfner is acknowledged as well as financial support from the Stichting voor Fundamenteel Orderzoek der Materie.

[a]Current address: Lyman Laboratory of Physics, Harvard University, Cambridge, Mass. 02138.

[1]For a review, see I. F. Silvera, Physica (Utrecht) 109&110B+C, 1499 (1981).

[2]I. F. Silvera and J. T. M. Walraven, Phys. Rev. Lett. 44, 164 (1980).

[3]R. W. Cline, T. J. Greytak, and D. Kleppner, Phys. Rev. Lett. 47, 1195 (1981).

[4]R. Sprik, J. T. M. Walraven, G. H. van Yperen, and I. F. Silvera, Phys. Rev. Lett. 49, 153 (1982).

[5]B. W. Statt and W. N. Hardy, private communication, have reported preliminary high-field ESR results.

[6]J. T. M. Walraven and I. F. Silvera, Phys. Rev. Lett. 44, 168 (1980).

[7]T. Niinikoski and L. Dick, private communication.

[8]N. S. Nishioka, P. L. Richards, and D. P. Woody, Appl. Opt. 17, 1562 (1978).

[9]B. W. Statt and A. J. Berlinsky, Phys. Rev. Lett. 45, 2105 (1980).

[10]A. J. Berlinsky and R. W. Cline, private communication.

High-Resolution X-Ray Scattering Study of the Nematic-to-Smectic-*C* Transitions in $\overline{8}$S5-$\overline{7}$S5 Mixtures

C. R. Safinya

Department of Physics, Massachusetts Institute of Technology, Cambridge, Massachusetts 02139, and Corporate Research Laboratories, Exxon Research and Engineering Company, Linden, New Jersey 07036

and

L. J. Martínez-Miranda, M. Kaplan,[a] J. D. Litster, and R. J. Birgeneau

Department of Physics and Center for Materials Science and Engineering, Massachusetts Institute of Technology, Cambridge, Massachusetts 02139

(Received 8 March 1982)

Measurements of the mass-density fluctuations associated with the first-order nematic–to–smectic-*C* transitions in $\overline{8}S5_{1-x}$-$\overline{7}S5_x$ mixtures are reported. This binary system exhibits nematic, smectic-*A*, and smectic-*C* phases, and a multicritical point x_{NAC}. As a function of decreasing temperature for $x > x_{NAC}$, the scattering in the nematic phase evolves from smectic-*A* to pretransitional smectic-*C* fluctuations described by a Lifshitz model of Chen and Lubensky. Important discrepancies remain with the predictions of the model near x_{NAC}.

PACS numbers: 61.30.Eb, 64.70.Ew

The nematic–to–smectic-*A* (NA) transition has been studied in considerable detail.[1] On the other hand, very little accurate information is available on the NC transition, and indeed the global nature of the entire multicritical NAC region where the NA and NC lines meet is not understood. To elucidate the problem, we have carried out a high-resolution x-ray scattering study of the critical mass-density fluctuations associated with the nematic–to–smectic-*C* transition in mixtures of octyl and heptyl oxy-*p*′-pentyphenylthiolbenzoate ($\overline{8}S5_{1-x}$-$\overline{7}S5_x$). By approaching x_{NAC}, one is able to study the transition as the tilt angle and latent heat are continuously decreased along the NC line; this line terminates at a second-order multicritical point at concentration x_{NAC}, and branches off into second-order nematic–smectic-*A* and smectic-*A*–smectic-*C* lines (Fig. 1). The NAC problem has two features which make it a prototype for problems of broad interest. First, in the de Gennes[2] description of an infinite-dimensional density order parameter, the NC system

